

**FIGURE 26.** Top:  $^{18}\text{F}$ -ML-10 uptake on PET at d 9 after whole-brain radiation therapy for metastases from non-small cell lung cancer in (top) a patient who responded well with a 63.1% voxel increase over baseline and (bottom) a patient who responded with a 36.7% voxel increase over baseline. At 2 mo, these patients showed respective tumor shrinkages of 57% and 18% on MR imaging.

future in the form of combined instruments and is already important with separate instruments and images later coregistered and combined.

### Conclusion: Highlights in Oncology

I see a growing potential for targeted radiotherapy with new natural and artificial carriers. We will see an abundance of agents that target a variety of molecules in cancer, and these will be based on platforms that can be easily manufactured, easily regulated, and (hopefully) more rapidly approved. We will see novel radionuclides, such as the  $\alpha$  emitters and a continuing variety of  $\beta$  emitters. A huge potential remains for further exploiting the phenotype of malignancy (which is a window on the biology of cancer) for diagnosis and staging and especially for looking at treatment response. I must admit that I removed some slides on biomarkers from this presentation, because I felt that the quality of the studies was not optimal. We must become more serious about biomarker studies. We cannot do that alone in individual institutions, because it takes many hundreds of patients and very well designed studies to actually convince the FDA that we have a valuable agent that will advance patient management.

Radiotracers for cancer pharmacology will also be an important part of our future, and already industry groups have set up large nuclear medicine units where they are looking at drugs, often labeled with  $^{11}\text{C}$ , as a way to get information of value for planning further development of clinical trials.

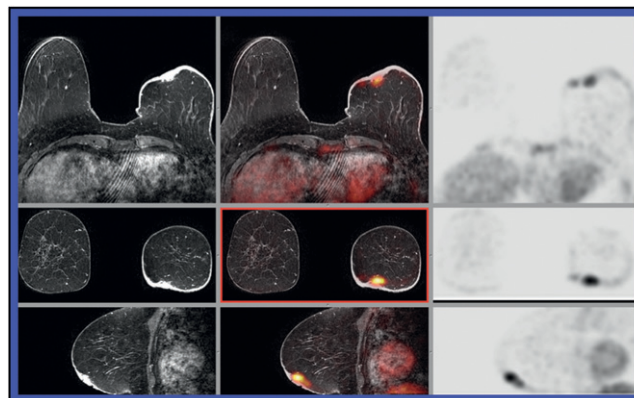


**FIGURE 27.** Images acquired with MR (left) and PET (right) in a patient with breast cancer are coregistered (middle).

The power of PET has greatly exceeded that of SPECT. I want to challenge imaging physicists to continue working to quantitate SPECT. This is apparently a very big challenge, because SPECT is now far behind PET in this regard. SPECT would have some advantages over PET if we could just label 2 radiopharmaceuticals, for example, and image them simultaneously.

We are also currently witness to the increasing power of chemistry to exploit improved knowledge of biology for novel radiotracers for oncology. This is an area in which the Department of Energy has continued its historical commitment by training chemists and radiochemists. The radiochemists have been an important part of our discipline. Nuclear medicine exists because of 3 components: the physicians, the radiochemists, and the medical physicists.

In addition, we must have an increasing emphasis on quantification, including kinetic modeling and dynamic imaging. As I mentioned, imaging biomarker studies are in their infancy and are grossly underpowered. I applaud the work of Michael Graham, MD, PhD, who in his year as SNM president worked very hard to create a vital clinical trials group within the society. We must continue to work together, both nationally and internationally, to bring the best tracers to the point of clinical use for the benefit of our patients.

*Steven M. Larson, MD  
Memorial Sloan-Kettering Cancer Center  
New York, New York*

## General Nuclear Medicine

The Scientific Program Committee defined general nuclear medicine to include a number of subcategories: endocrinology, gastroenterology, oncology (general practice),  $^{18}\text{F}$ -FDG, therapy, hematology/infectious disease, musculoskeletal, operations/outcomes research, pediatrics, pulmonary, and renal electrolyte/hypertension. This talk covers most of these subcategories. About 190 abstracts were accepted in the areas of general clinical nuclear medicine, and the categorical breakdowns are graphed in Figure 28.

I attempted to spot trends in scientific sessions and presentations at this meeting. One was the rise in SPECT/CT (with data shown in the second part of Figure 28). I expect this trend of

increasing numbers of presentations on SPECT/CT at this meeting to continue.

Han et al. [541] from Glasgow University and Glasgow Royal Infirmary (UK) reported on the “Clinical impact of SPECT/CT bone scan in assessment of bone metastases in breast cancer.” This group studied 449 patients, in 23% of whom the studies were inconclusive with planar imaging. Most of these patients underwent SPECT/CT, and the in-



**Harvey A. Ziessman, MD**

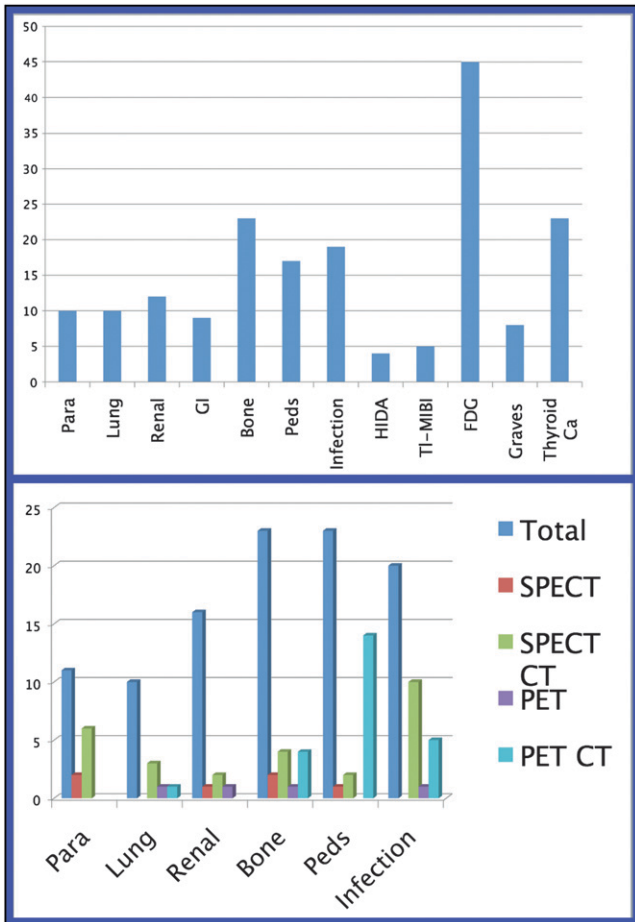


**FIGURE 28.** Scientific presentations on general nuclear medicine topics at 2010 SNM Annual Meeting. Top: general nuclear medicine topics represented. Bottom: Number of SPECT, SPECT/CT, PET, and PET/CT presentations for various subject categories.

conclusive rate went down to 1%. The authors found that SPECT/CT (with sensitivity, specificity, and accuracy of 94%, 97%, and 91%, respectively) improved localization and helped detect lytic lesions. Figure 29 is an example from the study. Uptake in the upper spine on planar imaging in this patient was poorly localized. SPECT/CT showed fusion of the bone scan uptake with the lytic lesion in the spine on CT, consistent with a metastasis.

Gourevich et al. [92] from Rambam Health Care Campus and the Technion–Israel Institute of Technology (in Haifa, Israel) reported on “SPECT/CT, an adjunct to bone scintigraphy: referral patterns and clinical value.” The authors considered SPECT/CT as an adjunct to scintigraphy and looked at 135 SPECT/CT studies. They found that the most common indications were to differentiate bone from soft tissue uptake and to better localize the uptake. SPECT/CT improved diagnostic accuracy in 54% of patients and guided additional imaging and invasive procedures in 17%. Figure 30 shows a patient with low back pain who had poorly localized lumbar spine uptake on whole-body imaging. SPECT/CT showed that the uptake localized to sclerotic CT bone changes consistent with degenerative joint disease.

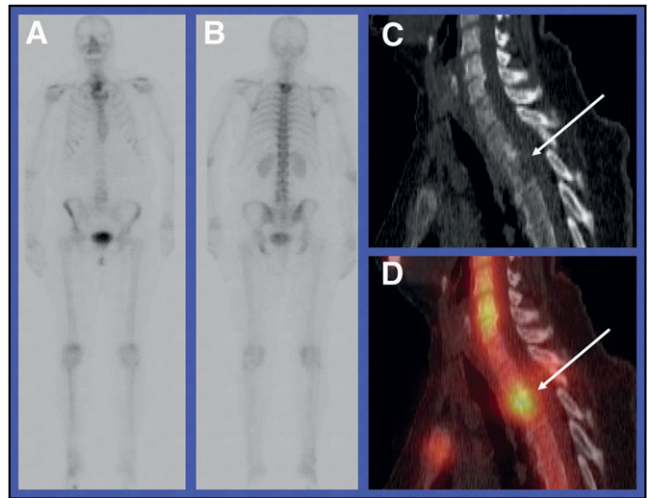


**FIGURE 29.** SPECT/CT in assessment of bone metastases in breast cancer. 58-y-old patient was 4 y postsurgery and radiation therapy and reported back pain. SPECT/CT showed that the <sup>99m</sup>Tc-MDP uptake fused with destruction of T2 seen on CT. This was followed by decompression surgery and radiation therapy.

Djekidel et al. [372] from the University of Michigan (Ann Arbor) reported on the “Benefits of hybrid SPECT/CT for <sup>111</sup>In-oxine- and <sup>99m</sup>Tc-HMPAO-labeled leukocyte imaging.” In 134 patients with a total of 221 lesions, SPECT/CT (with sensitivity, specificity, and positive and negative predictive values of 87%, 83%, 81%, and 89%, respectively) increased the number of correctly identified lesions by 27%. The authors particularly noted that SPECT/CT increased reader confidence by a large degree over planar imaging. Figure 31 shows whole-body planar images and SPECT in 1 of these patients, with poorly localized uptake in the anterior chest. SPECT/CT, however, clearly showed that this patient had an infected right ventricular pulmonary conduit.

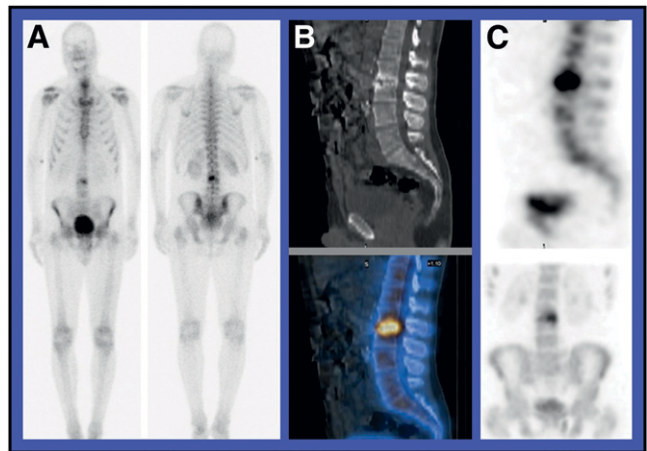


**FIGURE 30.** SPECT/CT as an adjunct to scintigraphy. 54-y-old man with low back pain and poorly localized lumbar spine uptake on whole-body imaging (A). SPECT/CT (B) showed uptake localized to sclerotic CT bone changes consistent with degenerative joint disease (inferior L2/superior L3).

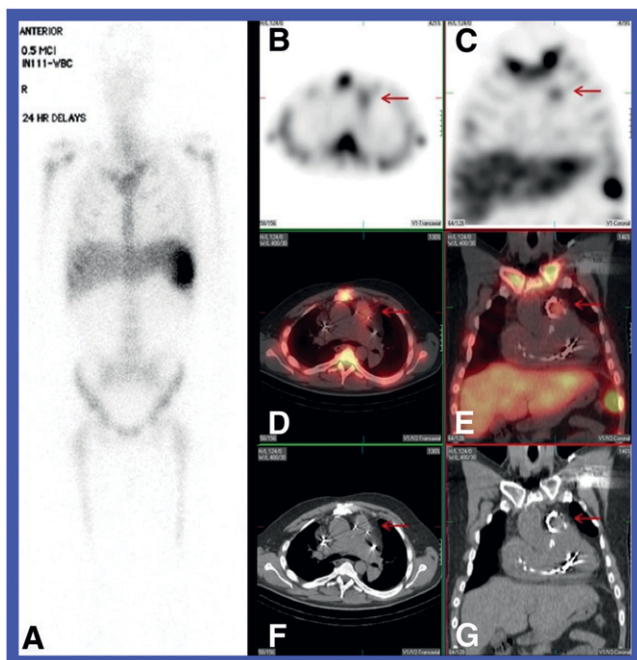


**FIGURE 31.** SPECT/CT for  $^{111}\text{In}$ -oxine-labeled leukocyte imaging. Whole-body planar images (A) and SPECT (B and C) showed poorly localized uptake in the anterior chest. CT (F and G) showed a right ventricular pulmonary conduit. Fused SPECT/CT (D and E) confirmed an infected conduit and endocarditis.

We continue to seek an infection imaging agent that does not require labeling the blood components. Singh et al. [373] from the Postgraduate Institute of Medical Education and Research (Chandigarh, India) and the Defence Research and Development Organization (Delhi, India) reported on “Clinical efficacy of a single-vial kit preparation of  $^{99\text{m}}\text{Tc}$ -ceftriaxone (Scintibact) for diagnosis of orthopedic infections: first results.” With this radiolabeled third-generation cephalosporin, the authors were able to detect hip prosthesis infections in 11 of 14 patients (with sensitivity, specificity, and accuracy of 80%, 75%, and 71%, respectively) (Fig. 32).

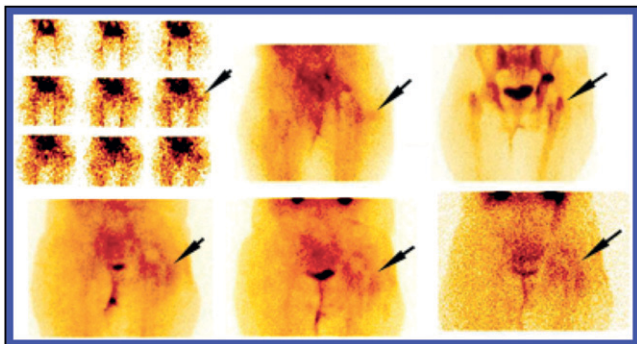


**FIGURE 32.** Imaging with a radiolabeled third-generation cephalosporin. Top row, left to right:  $^{99\text{m}}\text{Tc}$ -MDP perfusion, blood pool, and 3-h-delay scans. Bottom row, left to right:  $^{99\text{m}}\text{Tc}$ -ceftriaxone scans at 1, 4, and 24 h. Arrows point to patient's infected right hip prosthesis.

Another approach was described by Graute et al. [1630] from the Ludwig-Maximilians-Universität München (Germany), who reported on “Detection of low-grade joint infections using  $^{99\text{m}}\text{Tc}$ -antigranulocyte SPECT/CT: initial clinical results.” They looked at the detection of low-grade joint infections in 31 patients. All patients underwent  $^{99\text{m}}\text{Tc}$ -antigranulocyte planar scintigraphy at 5 min, 5 h, and 24 h after injection, as well as SPECT/CT at 6 h after injection. SPECT/CT results were compared with planar imaging alone and planar imaging with SPECT, and findings were evaluated against a gold standard of clinical data, including bacteriologic cultures, cell scores in joint aspirate, C-reactive protein, operative findings, and clinical follow-up. SPECT/CT was found to provide the highest accuracy for anatomic localization and determination of extent of infection. It was useful in selection of patients requiring surgical intervention. In Figure 33, planar imaging at all time points showed poorly localized uptake, whereas SPECT/CT showed the infection extending along the medial aspect of the left knee prosthesis.

I was surprised to see an abstract on  $^{67}\text{Ga}$  for infection imaging, but this was such a remarkable set of SPECT/CT images that I had to include them (Fig. 34). Caillat-Vigneron et al. [93] from the Hotel Dieu Hospital (Paris, France) reported on “ $^{67}\text{Ga}$  SPECT-CT imaging in diabetic foot: a confrontation with the results of bedside bone biopsy.” Thirty-eight of 51 patients had focal bone uptake adjacent to ulcers, and these patients responded to antibiotics. The authors felt that SPECT/CT was quite valuable in diagnosing osteomyelitis adjacent to foot ulcers.

In the future we more likely will be using  $^{68}\text{Ga}$ -citrate, a generator-produced positron emitter, in imaging infectious disease. Nanni et al. [368] from the Orsola Malpighi Hospital (Bologna, Italy) and the Santa Maria della Misericordia Hospital (Rovigo, Italy) reported on “ $^{68}\text{Ga}$ -citrate PET/CT in patients with inflammation/infectious disease.” They reviewed the studies of 47 patients and found that  $^{68}\text{Ga}$  PET/CT had high accuracy for the diagnosis of infection (sensitivity, specificity, positive and negative predictive values, and accuracy of 93%, 83%, 90%, 88%, and 89%, respectively). Figure 35 is an example of infection before therapy and resolution after therapy.

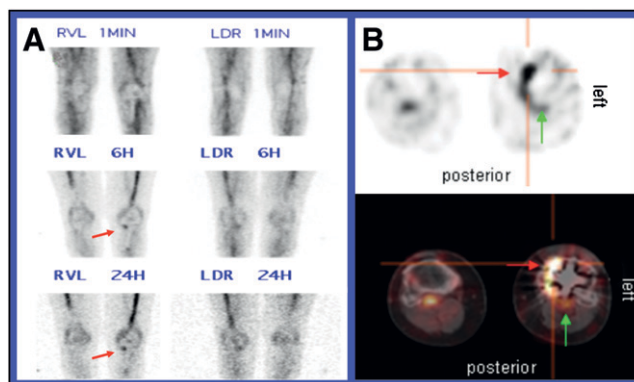


**FIGURE 33.** Imaging of low-grade joint infections. 61-y-old woman with total knee prosthesis on left side, with post-operative pain and *Lactobacillus gasseri* isolated in needle aspiration. SPECT/CT (B, bottom) added to information provided by planar (A) and SPECT (B, top) imaging by pinpointing the location of the infection (red arrow) and indicating that infection extended along the medial aspect of the patient's prosthesis (green arrow).

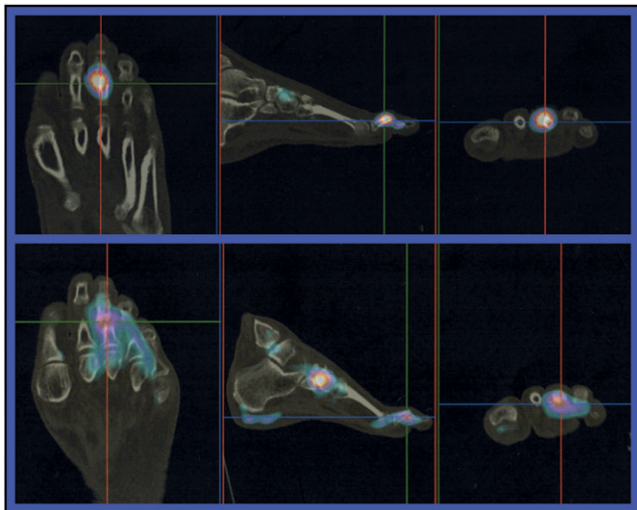


**FIGURE 34.**  $^{67}\text{Ga}$  SPECT/CT imaging in the diabetic foot. Patient with focal bone uptake adjacent to foot ulcer responded to antibiotics for osteomyelitis. Top row: before antibiotic therapy. Bottom row: 4 mo after antibiotic therapy shows resolving infection.

Lu and Schoder [39] from the Memorial Sloan-Kettering Cancer Center (New York, NY) reported on “Comparison of noncontrast perfusion SPECT-CT and planar V/Q in diagnosing acute pulmonary emboli (PEs) in patients with contraindications for CT angiography.” The study included 41 patients with Wells scores  $\geq 7$  who underwent same-day planar and  $^{99\text{m}}\text{Tc}$ -

macroaggregated albumin perfusion noncontrast SPECT/CT. For SPECT/CT the criterion for PE was  $>50\%$  segmental perfusion defect without CT abnormality. Prospective Investigation of Pulmonary Embolism Diagnosis criteria were used for planar imaging. The authors found that SPECT/CT had vastly superior sensitivity for PEs compared with planar V/Q (100% and 40%, respectively), although SPECT/CT was inferior to planar imaging in specificity (88% and 96%, respectively). In Figure 36, planar images do not clearly show a perfusion abnormality; however, segmental perfusion defects are clearly shown on SPECT/CT in the right middle lobe and in basal segments.

Ilic et al. [1669] from the Centre Hospitalier Universaire Vaudois (Lausanne, France), Université François Rabelais de Médecine (Tours, France), and Fribourg Hospital (Switzerland) reported on “SPECT/CT study of human bronchial particle deposition in human volunteers in a model of vaccination by aerosol.” The authors investigated vaccination by aerosol inhalation in order to deliver the antigen to the mucosal tissue of the proximal bronchi. They used SPECT/CT to assess and quantify regional distribution of the antigen in 20 healthy volunteers (Fig. 37). The study provided optimized deposition parameters for particle inhalation vaccination. They noted that this technique would be particularly useful in third-world countries.

Santi et al. [540] from the Università di Bologna (Italy) and the Technische Universität München (Germany) reported on “Freehand SPECT for sentinel lymph node biopsy: first clinical experience.” Their aim was to evaluate SPECT accuracy with this handheld device in detection and localization of sentinel lymph

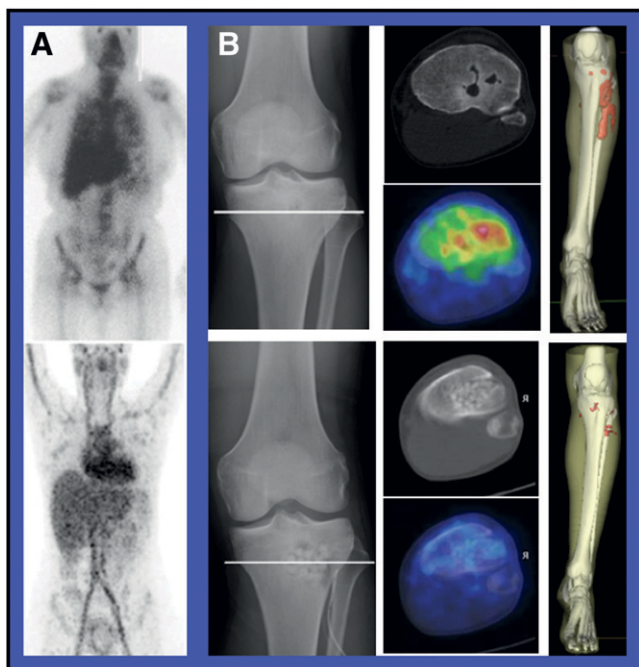


**FIGURE 35.** (A)  $^{67}\text{Ga}$  (top) and  $^{68}\text{Ga}$  (bottom) -citrate imaging showing normal uptake. (B) Imaging in acute osteomyelitis of the tibia before (top set of images) and after (bottom set of images) therapy. Left: plane radiographs. Middle: Transaxial CT (above) and PET (below). Right: Fused  $^{68}\text{Ga}$ -citrate PET/CT volume display.

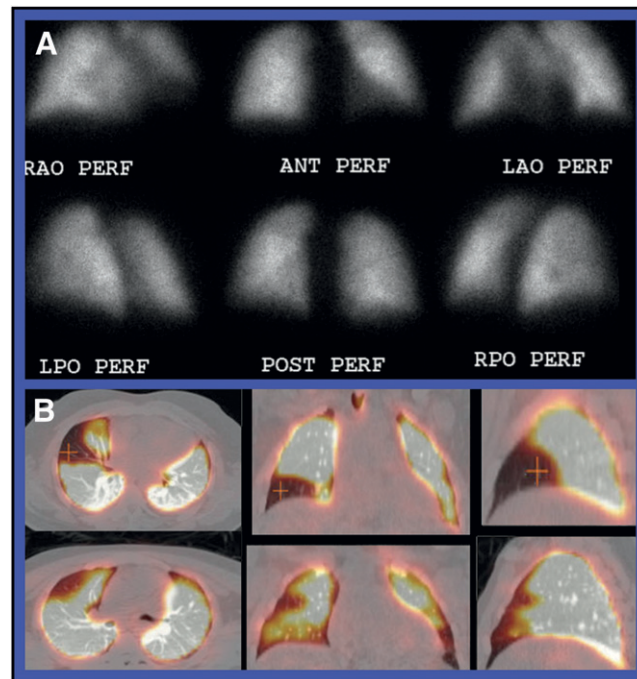


**FIGURE 36.** Noncontrast perfusion SPECT/CT vs planar V/Q in acute pulmonary embolism (PE). 51-y-old man with renal cell cancer, renal insufficiency, dyspnea, and chest pain on postoperative day 1. Top: planar V/Q images do not clearly show a perfusion abnormality. Bottom: SPECT/CT shows segmental perfusion defects in the right middle lobe and in basal segments.

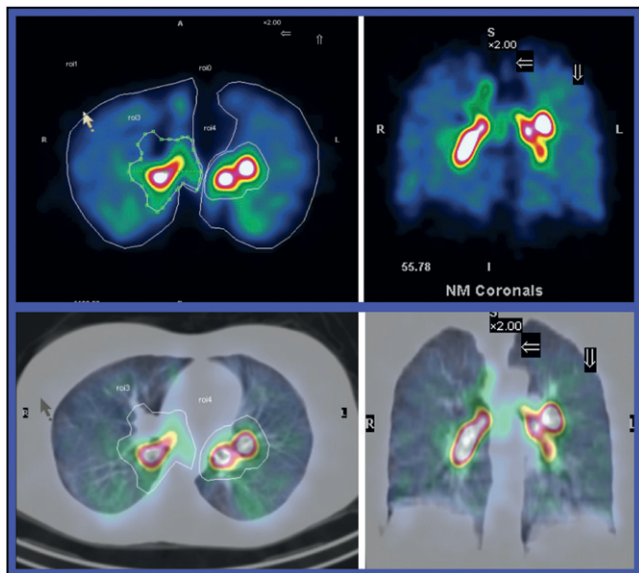


**FIGURE 37.** SPECT/CT of human bronchial particle deposition in a model of aerosol inhalation vaccination assessed and quantified regional distribution of administered antigens in healthy volunteers.

nodes in breast cancer. The study included 50 patients with invasive breast cancer who received 60–80 MBq  $^{99m}\text{Tc}$ -nanocolloid and underwent freehand SPECT imaging (Fig. 38). SPECT identified at least 1 lymph node in 49 of the 50 patients (98% sensitivity),

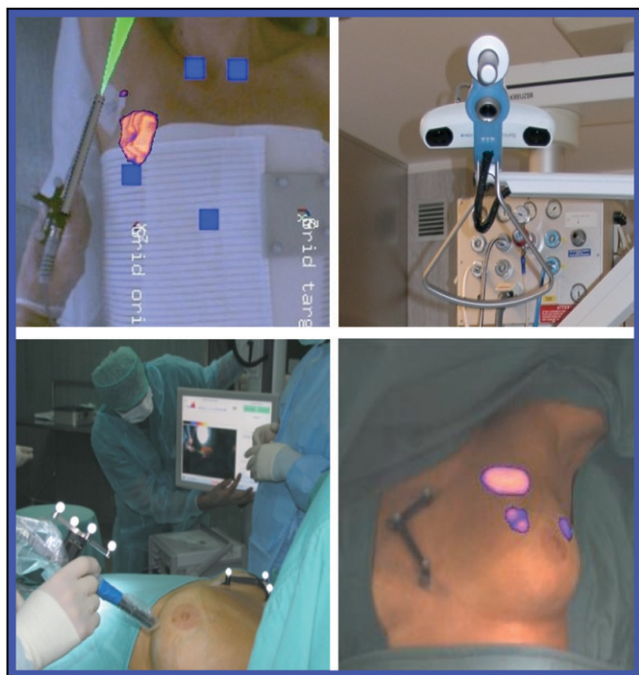


**FIGURE 38.** Freehand SPECT for sentinel lymph node biopsy. Top left: freehand overlaid on video. Bottom right: Light patch indicates injection site, right purple spot indicates sentinel lymph node. The technique accurately localizes sentinel lymph nodes in the axillae, providing intraoperative 3D information to surgeons.

whereas planar imaging identified 76 of 91 lymph nodes (84% sensitivity). They concluded that freehand SPECT is able to accurately localize sentinel lymph nodes in the axilla, providing useful 3D information for surgeons for lymph node dissection.

McCauley et al. [258] from the Brigham and Women's Hospital/Harvard Medical School (Boston, MA) reported that “FDG uptake does not distinguish malignant from benign pleural effusions.” They looked at 42 patients with large pleural effusions (half malignant and half benign) and calculated standardized uptake values (SUVs) for the effusions and effusion/lung ratios and found that these metrics could not distinguish malignant from benign pleural effusions (Fig. 39).

Dierickx et al. [257] from the Institut Claudius Regaud, the Centre Hospitalier Universitaire Rangueil and Paul de Viguier hospitals, and the Clinique St. Jean Languedoc (all in Toulouse, France) reported on “Correlation of PET/CT with  $^{18}\text{F}$ -FDG and male fertility.” The authors looked at  $^{18}\text{F}$ -FDG uptake in early spermatocytes and spermatozooids in 20 men with a mean age of 22 y (Fig. 40). They found significant correlation between testicular uptake and parameters of spermograms, such as sperm count. They concluded that  $^{18}\text{F}$ -FDG PET/CT may have clinical applications in the diagnosis and prognosis of hypofertility and infertility.

Nakada et al. [200] from Hokko Memorial Hospital, Kaisei Hospital, and Hokkaido University Hospital (Sapporo, Japan) reported on the “Clinical value of fusion images of MIBI SPECT and enhanced multidetector CT (MDCT) registered by workstation in primary hyperparathyroidism.” The prospective study included 31 individuals with primary hyperparathyroidism who underwent both MIBI SPECT imaging and MDCT angiography on the same day. Each patient underwent early 20-min and delayed 120-min MIBI planar and SPECT imaging, followed by 64-row MDCT with contrast enhancement. Data were subsequently 3D volume rendered to produce images that generated not only the sestamibi image in 3 dimensions but also clearly showed the feeding arteries. Fusion imaging identified 32 parathyroid abnormalities (94%) in these individuals, better than either SPECT alone or ultrasound (each at 79%). Fusion imaging showed the feeding arteries in 29 glands. The images in Figure 41 are quite remarkable. The normal thyroid is seen in yellow. The gray area is a thyroid adenoma with a superior thyroid artery feeding vessel. In the posterior view, the parathyroid adenoma is green and a feeding vessel is visualized coming off the internal mammary artery from the brachiocephalic trunk. In Figure 42, with the sestamibi bright blue, the parathyroid adenoma is seen

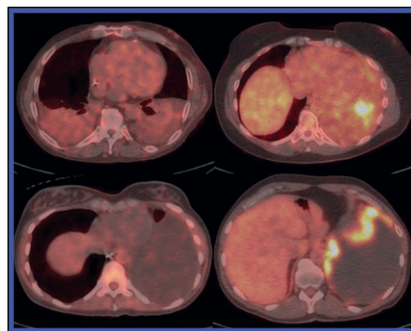


**FIGURE 39.** Images from datasets acquired in patients with benign (left) and malignant (right) pleural effusions. The images on the right show a range of  $^{18}\text{F}$ -FDG uptake. At top right, the  $\text{SUV}_{\text{avg}}$  was 2.1; at bottom,

the patient was relatively photopenic, with an  $\text{SUV}_{\text{avg}}$  of 0.6. On the left, the benign pleural effusions show SUV values within this same range, indicating that  $^{18}\text{F}$ -FDG uptake cannot distinguish benign from malignant pleural effusions.

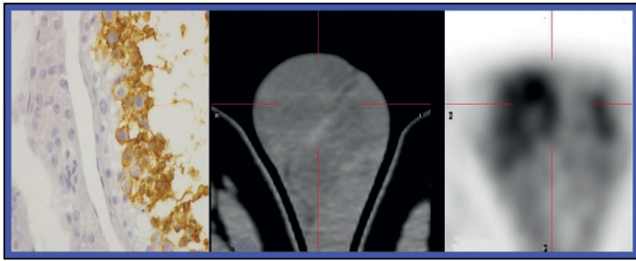


**FIGURE 40.**  $^{18}\text{F}$ -FDG uptake in early spermatocytes and spermatozoa. The authors found correlation between testicular uptake and parameters such as sperm count, suggesting that  $^{18}\text{F}$ -FDG PET/CT may have applications in diagnosis and prognosis of hypofertility and infertility.

as green, inferior and posterior to the thyroid, with the inferior thyroid artery as the feeding vessel. [Editor's note: This image was subsequently chosen as the 2010 SNM Image of the Year.] The authors believed this could be very useful for preoperative surgical planning, and I agree.

Umlauf et al. [146] from the University of Washington Medical Center (Seattle) and the Seattle Cancer Care Alliance (WA) looked at " $^{131}\text{I}$  therapy in differentiated thyroid cancer (DTC) using recombinant human thyroid stimulating hormone (rhTSH): Biokinetic data and proposed dosing scheme." They accessed 169  $^{131}\text{I}$  dosimetry measurements in patients with DTC and calculated whole-body retention at 48 h, whole-body retention time, retention in the blood at 48 h, blood residence time, peak blood dose, and creatinine clearance rates after either rhTSH stimulation or thyroid hormone withdrawal. They found significantly faster clearance of  $^{131}\text{I}$  for rhTSH than for thyroid hormone withdrawal, which was not surprising, because hormone withdrawal reduces the glomerular filtration rate (GFR). However, they used this quantitative data to propose an empiric formulation for adjusting dose for rhTSH stimulation based on GFR.

Bural et al. [489] from Children's Hospital/Harvard Medical School (Boston, MA) reported on "Thymic uptake of radioiodine

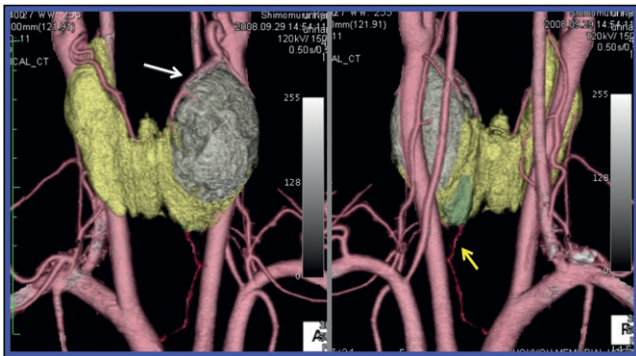
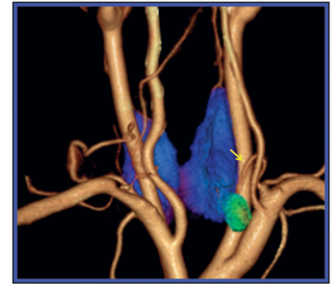


**FIGURE 41.** 3D volume rendering of CT of arteries in the neck, thyroid gland, and enlarged parathyroid gland from the anterior (left) and posterior (right) projection in a female patient with a parathyroid adenoma and follicular adenoma of the thyroid. Normal thyroid is seen in yellow. The gray area is a thyroid adenoma with a superior thyroid artery feeding vessel. In the posterior view, the parathyroid adenoma is light green and a feeding vessel is visualized coming off the internal mammary artery from the brachiocephalic trunk.

**FIGURE 42.** Posterior aspect of coregistered image of volume-rendering CT angiography and 3D volume image in patient seen in Figure 41. Thyroid gland and parathyroid adenoma are rendered in blue and green, respectively. This image was chosen as the SNM 2010 Image of the Year.



in children and young adults with thyroid cancer." In 55 patients treated with radioiodine and evaluated before and after therapy, the authors showed that thymic uptake is fairly common, particularly after therapy, and emphasized the importance of not confusing this uptake with metastatic disease.

Beyer et al. [260] from cmi experts (Zurich, Switzerland), the University of California at Los Angeles, and University Hospital Essen (Germany) reported on "Variations of clinical PET/CT operations for oncology imaging: an international Web-based survey." They surveyed 100 PET/CT centers with a 50-item questionnaire on clinical protocols used. The conclusion from the data they collected was that significant variations exist in  $^{18}\text{F}$ -FDG PET/CT protocols, emphasizing the need not only for additional training but for standardization.

Fig et al. [594] from the Veterans Affairs (VA) Healthcare System (Ann Arbor, MI), New York University (NY), and the University of Utah (Salt Lake City) asked the question "Are national guidelines incorporated into local myocardial perfusion imaging protocols?" This was a study of 131 VA hospital nuclear medicine laboratories provided with myocardial perfusion imaging (MPI) phantoms with simulated stress/rest defects on which each lab performed its own SPECT MP protocol. The authors found wide variations in the protocols used and concluded that national guidelines are not routinely followed at many sites.

Bhambhani et al. [597] from the University of Alabama at Birmingham reported on "Variability in cholescintigraphy (HIDA) protocols in hospitals across the state of Alabama." The authors surveyed 51 nuclear medicine departments in hospitals and found wide variability in patient preparation and hepatobiliary iminodiacetic acid protocols. These varied most widely in length of sincalide infusion, gall bladder ejection fraction values, and pretreatment with sincalide. They concluded that wide protocol variability, although assessed in Alabama alone, is likely to be common in other states.

I want to conclude by noting that the SNM has a new council: the General Clinical Nuclear Medicine Council. This was previously the Gastrointestinal Council. The council has been very involved in the standardization of imaging protocols (e.g., solid gastric emptying and sincalide infusion). We have now expanded our areas of interest to include all of general nuclear medicine. We would like to encourage all who are interested in general nuclear medicine to join the council.

Harvey A. Ziessman, MD  
Johns Hopkins University  
Baltimore, Maryland